Optimised exfoliation conditions enhance isolation and solubility of grafted graphenes from graphite intercalation compounds

Takuya Morishita,[a,b] Adam J. Clancy[a] and Milo S. P. Shaffer*[a]

In bulk applications, it is essential that graphene sheets disperse individually in solvents or matrices, and therefore, suitable functionalisation regimes are crucially important. Here, isolated, highly soluble, alkyl-grafted graphenes were synthesised by reacting exfoliated Na-reduced graphite intercalation compounds (GIC) with alkyl halides. In this reaction, efficient exfoliation of the Na-reduced GICs into individually-dispersed negatively-charged graphenes provides accessible surface area for grafting. Increasing the alkyl chain length leads to large decrease of the grafting ratio (GR), demonstrating that steric factors also play an important role. However, optimising the Na concentration (C/Na ratio) in the reaction was very effective for improved exfoliation and increased GR. The X-ray diffraction measurements suggest that particular C/Na ratios (C/Na = ~12) led to full exfoliation, by balancing total charge and charge condensation effects and that the GR can be significantly increased even in the case of long alkyl chains (eicosyl chains), corresponding to a high solubility of 37 μg ml^{-1} and high yield in *o*-dichlorobenzene. Moreover, the absolute Na concentration is the critical parameter, with the same optimum (~0.01 M) for exfoliation and grafting of GIC at all graphite concentrations; it was possible to graft even at high graphite concentration (0.3 M (3.6 mg ml^{-1})) successfully.

1. Introduction

Graphenes are attracting immense attention for a wide range of promising potential applications.[1–8] Graphene sheets have been prepared by micromechanical cleavage of graphite,[2] epitaxial growth,[9] chemical vapor deposition,[10] organic synthesis[11] and carbon formation.[8] In many applications, such as nanocomposite materials,[1–5] electronic inks,[2,3] flexible displays,[3] drug delivery[2,4] and sensors,[3] the individual graphene layers must be dispersed in solvents or matrices by a scalable method. However, pure graphene has only low solubility in common solvents;[12] functionalisation is crucial to avoid restacking and enable processing, in many practical bulk situations. The production of graphene oxide[4,5,13,14] by acid exfoliation is popular but damages the intrinsic structure and degrades properties. Alternative, milder wet-chemical approaches generate graphenes from graphites by exploiting exfoliation and stabilisation using carefully selected surfactants or solvents.[12,15,16] However, such graphenes typically involve extended sonication which leads to formation of structural defects and reduced flake size.[16] The best approach to retain the bonded network and the lateral dimensions of graphenes involves the formation of electrostatically-stabilised dispersions by protonation in superacids[17] or reduction and dissolution in polar aprotic solvents.[18,19] Examples include intercalation of graphite with liquid potassium-ammonia[18] followed by dissolution in tetrahydrofuran (THF), and the dissolution of potassium-based graphite intercalation compounds (GICs) in *N*-methyl pyrrolidone.[19] The resulting solutions contain individual solvated anionic graphenes (graphenides) as shown by small-angle neutron scattering[18] and are stable so long as air is excluded. Recently, covalent functionalisation of these graphenides has been achieved through reaction with a suitable electrophile.[20–22] This type of reaction using electrophiles such as alkyl halides was originally used for functionalisation of reduced SWNTs[23] and potassium graphites to produce functionalised graphites with 6-20 layers.[24] This approach has been adapted to produce functionalised graphene; for example, Na/K-reduced GICs were alkylated (hexylated) by reacting with 1-iodohexane in 1,2-dimethoxyethane.[21] In this reaction, a large excess of Na/K alloy and long times (7 days) were used for the reduction. However, the grafting ratio (GR) and solubility of the obtained hexylated graphenes were relatively low (e.g. GR: ~0.08, solubility: ~0.6 μg ml^{-1} in *o*-dichlorobenzene (DCB)).[21] In order to improve the GR, and hence the product solubility, the number of accessible negative charges on the reduced graphene must be increased. However, polyelectrolyte theory suggests a large excess of alkali metal will simply lead to increased condensation of the negative charges[25] causing 'salting out' rather than exfoliation of the graphene layers. In the case of alkali metal-reduced single-walled carbon nanotubes (SWNTs), it has been reported that increasing the counterion concentration increases the condensation of the charges and decreases the solubility.[26,27] By analogy, the control of alkali metal concentration (carbon/alkali metal ratio) in the graphene grafting reaction is expected to be a key step for better exfoliation and improved GR. This report considers the synthesis of isolated, highly soluble graphenes grafted with various alkyl chains. It demonstrates the importance of using particularly low metal content to improve exfoliation and increase grafting ratio by balancing total charge and charge condensation effects.

2. Experimental

2.1. Materials

Graphite (Graphexel natural crystalline flake graphite, grade: 2369, Graphexel Ltd., UK) was obtained from the manufacturer and used without any further purification. 1-Chlorododecane (>97%), 1-bromododecane (>98%) and 1-chloroeicosane (>96%) were purchased from Tokyo Chemical Industry Co., Ltd.. 1-Bromobutane (99%), 1-bromoeicosane (98%), 1-iododododecane (98%) and anhydrous THF were obtained from Sigma-Aldrich. 1-Chloroeicosane and 1-bromoeicosane were dried at room

temperature for at least 4 days under vacuum before using in the glove box. 1-Chlorododecane, 1-bromobutane, 1-bromododecane, 1-iodododecane and THF were degassed via a freeze-pump-thaw method and dried over 20% wt, molecular sieves 4A. Sodium (99.95%, ingot, No. 262714) and naphthalene (99%) were purchased from Sigma-Aldrich.

2.2. A typical example for synthesis of alkylated graphene

69 mg (3 mmol) of sodium and 384.5 mg (3 mmol) of dried naphthalene were added into 30 mL of degassed anhydrous THF in a N_2 filled glove box, and stirred for 1 day forming a green Na/naphthalene solution. A pre-made sodium naphthalide THF solution was used to allow for accurate, simple addition of sodium to the carefully dried graphite. Typically, a Schlenk tube including graphite (36 mg, 3 mmol of carbon) together with a magnetic bar was flame-dried, and placed in a glove box. A variable mass of the Na/naphthalene solution (1:1 in THF) was added into the Schlenk tube containing graphite and the concentration of graphite in THF adjusted to 0.1 M (mmol ml^{-1}) by addition of degassed anhydrous THF. The suspension was stirred for 1 day, and alkyl halides (9 mmol, 3 equiv. per sodium) were added to the tube. Then, the reaction was stirred at room temperature for 1 day under N_2. After bubbling dry O_2 into the solution for 15 min, the solution was stirred for 1 day under dry O_2 for oxidation of any remaining charges on the functionalised graphenes. The solution was stirred as ethanol (10 ml) was added slowly followed by water (20 ml). After neutralization using 0.1 N HCl, the functionalised graphenes were extracted into hexane and washed several times with water. The mixture was filtered through a 0.1 μm PTFE membrane filter, washed thoroughly with hexane, THF, ethanol and water. After washing the sample with ethanol and THF again, the product was obtained after drying overnight under vacuum at 80 °C.

2.3. Measurements

Thermogravimetric analysis (TGA) was performed using a Perkin Elmer Pyris 1 TGA under a well-controlled N_2 atmosphere (samples were held at 100°C for 90 min under N_2 flow of 60 ml min^{-1}, then ramped 10 °C min^{-1} to 800 °C). FT-IR spectra were measured using a Perkin Elmer Spectrum 100 with a universal ATR sampling accessary. X-ray powder diffraction (XRD) was recorded at a scan rate of 0.108°/s with the Cu Kα (1.542 Å) line using a PANalytical X'Pert PRO diffractometer. UV–vis-NIR absorption spectra were measured using a Perkin Elmer Lambda 950 UV/Vis spectrometer. Sonication was performed using an ultrasonic cleaner (USC300T, 80 W). Raman spectra of powder samples were measured using an ISA Jobin Yvon SPEX Raman spectrometer equipped with a 532 nm excitation laser source. Typical tapping-mode atomic force microscopy (AFM) measurements were taken using Bruker MultiMode 8 AFM. Samples for AFM were prepared by drop-casting dilute graphene-dispersed chloroform solutions on silica substrates.

3. Results and discussion

3.1. Synthesis of alkylated graphenes

Fig. 1 shows the synthesis of alkylated graphenes through *in situ* functionalisation of Na-reduced graphite with alkyl halides. Na and naphthalene were used as the electron source and transfer agent respectively, for the preparation of Na-reduced graphites. THF was selected as the solvent for its ability to coordinate sodium ions both in solution and between GIC layers. This solution process yields stage-1 Na-THF-GIC.[28,29] The presence of coordinated THF increases the interlayer spacing more effectively for sodium than potassium,[28] in this solution phase process. A pre-made sodium naphthalide THF solution was used to allow for accurate, simple addition of sodium to the carefully dried graphite. The resulting charged graphene sheets can be reacted with alkyl halides to yield exfoliated, grafted graphenes. A series of linear alkyl halides with varying lengths were explored as means to increase solubility. For example, eicosylated graphene (**1f**) was synthesised by the reaction of Na-reduced graphites with eicosyl halides. Thermogravimetric analysis (TGA) of **1f** in N_2 (Fig. S1) confirmed successful grafting. A pure eicosane control decomposed predominantly below 200°C with a small amount of char disappearing about ~550 °C. Graphite did not show any weight loss in the range from 100°C to 800°C (Fig. S1). Na-THF-GIC controls (after the same work-up procedure as **1f**) showed a relatively small weight loss from ~200°C to ~500°C (Fig. S2) and the amount of Na-THF-GIC remaining unreacted in **1f** was also small (Fig. S3)). Therefore, the weight loss observed in **1f**, at a higher temperature (>210°C) than pure eicosane, can be mainly attributed to grafted eicosyl chains, consistent with recent TGA-MS observations.[22] Based on this assumption, the average weight loss of eicosyl chains in **1f** was 14.6 wt% (Table 1) corresponding to a C/R ratio of 137. FT-IR spectra (Fig. 2a) include C-H stretching peaks (~2850 cm^{-1}–2960 cm^{-1}) attributed to the aliphatic chains of the grafted product (**1f**).

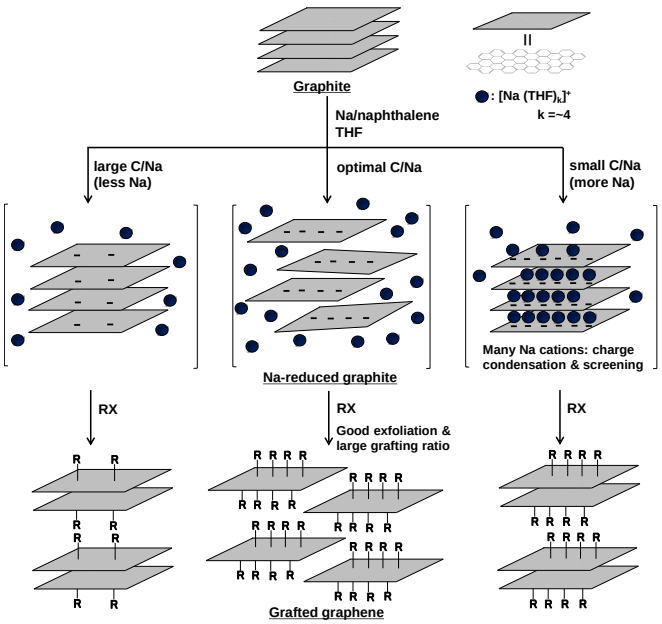

Fig. 1. Schematic representative of the synthesis of alkylated graphene using Na-reduced graphite. Bilayers represent unexfoliated stacks of two or more layers.

Further evidence of covalent functionalisation is obtained from Raman spectroscopy (Table 1 and Fig. 2b). The starting graphite was sufficiently crystalline that no D peak was visible. However, the D/G ratio of **1f** was 0.25 (Table 1); this significant increase is consistent with the formation of covalent bonds, as the grafted alkyl groups create sp^3 defects in the sp^2 framework. The shape of the 2D peak of **1f** (Fig. 2b), which is less asymmetric than the starting graphite, indicates partial exfoliation.[30] X-ray diffraction (XRD) measurements confirmed significant exfoliation of eicosylated graphene (Fig. 3a). Pristine graphite shows a strong interlayer (002) peak, however, the intensity of the (002) peak from an identically prepared sample was significantly reduced and broadened after the initial

eicosyl functionalisation (**1f**), indicating partial intercalation and exfoliation. In addition, a very small peak at $2\theta = 23.9°$ is characteristic of the (003) reflection of stage-1 Na-THF-GIC (Fig. S3).[28] Trapping of a proportion of the stage-1 structure is known to be possible even after exposure to air,[28] due to the preferential de-intercalation of the sheet edges.

Table 1 Properties of various alkylated graphenes.

code	RX	C/Na	weight loss[b)]	GR[c)]	C/R[d)]	D/G[e)]
1a	C_4H_9Br	1	12.8	0.147	32.4	0.67
1b	$C_{12}H_{25}Cl$	1	11.3	0.127	111.1	0.20
1c	$C_{12}H_{25}Br$	1	13.8	0.160	88.1	0.28
1d	$C_{12}H_{25}I$	1	17.0	0.205	68.9	0.31
1e	$C_{20}H_{41}Cl$	1	6.5	0.070	337.5	0.12
1f	$C_{20}H_{41}Br$	1	14.6	0.171	137.2	0.25
1g	C_4H_9Br	12	17.7	0.215	22.1	0.69
1h	$C_{12}H_{25}Br$	12	21.9	0.280	50.3	0.40
1i	$C_{12}H_{25}I$	12	23.2	0.302	46.8	0.41
1j	$C_{20}H_{41}Br$	12	23.0	0.299	78.5	0.30
1k	$C_{20}H_{41}Br$	24	18.1	0.221	107.1	0.24
1l[a)]	$C_{20}H_{41}Br$	12	23.3	0.304	77.2	0.34

[a)] Short bath-sonication (5min) was taken before adding RX.
[b)] Weight loss (wt%) of the alkyl chains estimated from TGA.
[c)] Alkyl chain/graphene mass ratios calculated using the weight loss.
[d)] Carbon/alkyl chain ratios of the obtained alkylated graphenes.
[e)] Average D/G ratios obtained by Raman measurements.

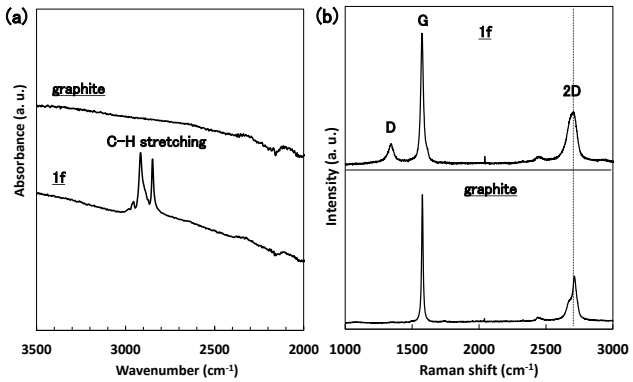

Fig. 2. (a) FT-IR spectroscopy of eicosylated graphene **1f** and pristine graphite.(b) Raman spectra (laser wavelength: 532 nm, normalised by the intensity of the G peak) of pristine graphite and eicosylated graphene **1f**.

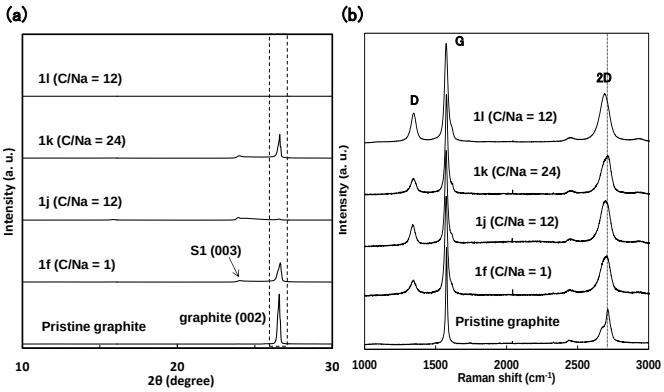

Fig. 3. (a) XRD patterns and (b) Raman spectra (laser wavelength: 532 nm, normalised by the intensity of the G peak) of pristine graphite and eicosylated graphenes **1f**, **1j**, **1k**, and **1l** (grafted after a brief bath sonication (5 min)).

3.2. Effect of halide species, alkyl chain length and stoichiometry

Encouraged by the initial successful eicosyl grafting reaction, further studies were performed to establish the effect of halide species, alkyl chain length, and stoichiometry. As shown in Table 1, a clear trend of increasing reactivity down the group of the order: RCl < RBr < RI was observed with alkyl iodides giving the greatest grafting Ratio (GR). The mechanism for the functionalisation of negatively-charged graphene with alkyl halides likely mirrors the radical reaction recently suggested for the addition of alkyl halides to K-reduced SWNTs,[31] and likely responsible for the hydrogenation of Li-reduced graphite using water.[32] As shown in Table 1 and Fig. 4a, decreasing the chain length led to a significant increase in the density of grafted chains (reduced number of graphene carbons per grafted chain, C/R). Butylated graphenes (**1g**) showed low C/R values, reaching as little as 22.1 graphene carbons per grafted chain. This trend demonstrates that steric factors play an important role in determining the outcome of these 'grafting to' reactions. In the theta state of a free-jointed linear polymer chain, the mean-square radius of gyration ($\langle S^2 \rangle$) is proportional[33] to the number of bonds (n) ($\langle S^2 \rangle = kn$). Therefore, the graphene area occluded by one grafting chain (C/R) might also be expected to be approximately proportional to n, as observed in the data (Fig. 4a). However, the conformation of the alkyl chains near the graphene is unknown and may vary as the reaction proceeds; the availability of the graphene surface and negative charge also vary with reaction conditions. In the case of well exfoliated C/Na = 12 samples (vide infra), for very short chains, the reaction appears to approach the limit of available charge (C/R = 12). For higher metal content systems (C/R = 1) the observed GR is unexpectedly lower, and more sensitive to the steric effects of chain length. This trend indicates a more limited surface area available for grafting which may be attributed to poorer exfoliation. A systematic study of the effect of the charge ratio on the degree of grafting (Fig. 4b) shows that the optimal C/Na ratio for maximum grafting density is ~12. As shown in Fig. 1, when the C/Na value is small, the total negative charge on the graphene is high, favouring Na-THF-GIC formation[28]; however, most of the charges are condensed and screened by the high concentration of Na cations.[25] This 'salting out' leads to incomplete exfoliation and lower GR, and is consistent with the assumption that grafting only occurs on exposed surfaces. In contrast, when the C/Na value is large, the total negative charge on the graphene is low, resulting in incomplete exfoliation and a low GR. Between these extremes lies an optimum for graphene exfoliation and grafting. As shown in Fig. 3a, both above (**1k**, C/Na = 24) and below (**1f**, C/Na = 1) this 12:1 ratio, the XRD diffractogram indicates remaining graphite as illustrated by the (002) peak. In contrast, at the optimal charge (C/Na = 12), the (002) diffraction of the alkylated graphene **1j** is almost absent. In these samples, a very small stage-1 peak (S1 (003) peak) originating from

remaining GICs was observed, probably due to physical connections between some layers limiting exfoliation. However, a brief weak sonication (5 minute bath-sonication) at the optimal charge ratio before the addition of eicosyl bromides led to apparently full exfoliation; the diffractogram does not show the graphite (002) peak and S1 (003) peak in the **1l** XRD data (Fig. 3a, Fig. S3b). The loss of the layer peaks can be explained by near full exfoliation into single layers; peak intensity can be affected by various factors, but all XRD samples were prepared and measured identically, in the same shape and volume: the only difference is the state of exfoliation and functionalisation. The 2D Raman peak for the C/Na = 12 samples (Fig. 3b, Fig. S4, samples **1j** and **1l**) is well-fitted by a single symmetric Lorentzian peak (R^2=0.99), shifted to lower frequency: this characteristic 2D peak is consistent with the existence of a single layer graphene sheet,[30] following full exfoliation, although the peak width is broader than for perfect graphene, as expected for functionalised material. [22,34]

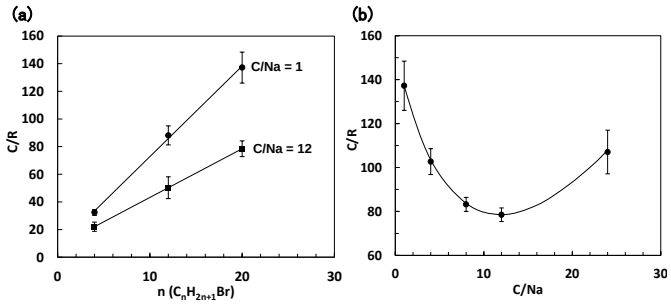

Fig. 4. (a) The relation between n number of $C_nH_{2n+1}Br$ used and the C/R value of the obtained C_nH_{2n+1} grafted graphenes, and (b) the relation between C/Na and C/R of eicosylated graphenes.

Further confirmation is provided by a tapping-mode atomic force microscopy (AFM) measurement of **1l** deposited onto silica from chloroform dispersion; the image (Fig. 5a) and the histogram (Fig. 5b) indicate that the eicosylated graphene product predominantly consists of functionalised single-layer sheets with average heights of 1.25 ± 0.2 nm. Nonfunctionalised single-layer graphenes are typically observed with the heights of ~0.8 nm on silica substrates,[35,36] and therefore, the grafted eicosyl chains are estimated to contribute ~0.45 nm in thickness to the graphene sheet (combining the GR and bulk density of eicosane would imply an alkane thickness of 0.3 nm, which can be expected to underestimate the true value due to the distribution of grafting sites preventing the formation of a fully dense layer). The narrow distribution of the thicknesses over a large number of flakes measured (standard deviation: 0.2 nm over 84 flakes), is much more consistent with experimental uncertainty and slight variations in grafting density, than multiple layers. Each additional graphene layer would add at least 0.3-0.4 nm, therefore, it seems unlikely that there is a significant contribution of few layer graphenes. The lateral dimensions of the eicosylated graphenes (~0.8 μm) are similar to the original graphite (the mean lateral size of the pristine graphite is ~1.0 μm (Fig. S5)), which is consistent with electrostatically-driven exfoliation and minimum framework damage. The D/G ratio (Table 1, Fig. 3b) of **1l** was not significantly greater than that of **1j**; the brief, weak, bath-sonication did not introduce significant defect formation or size reduction.

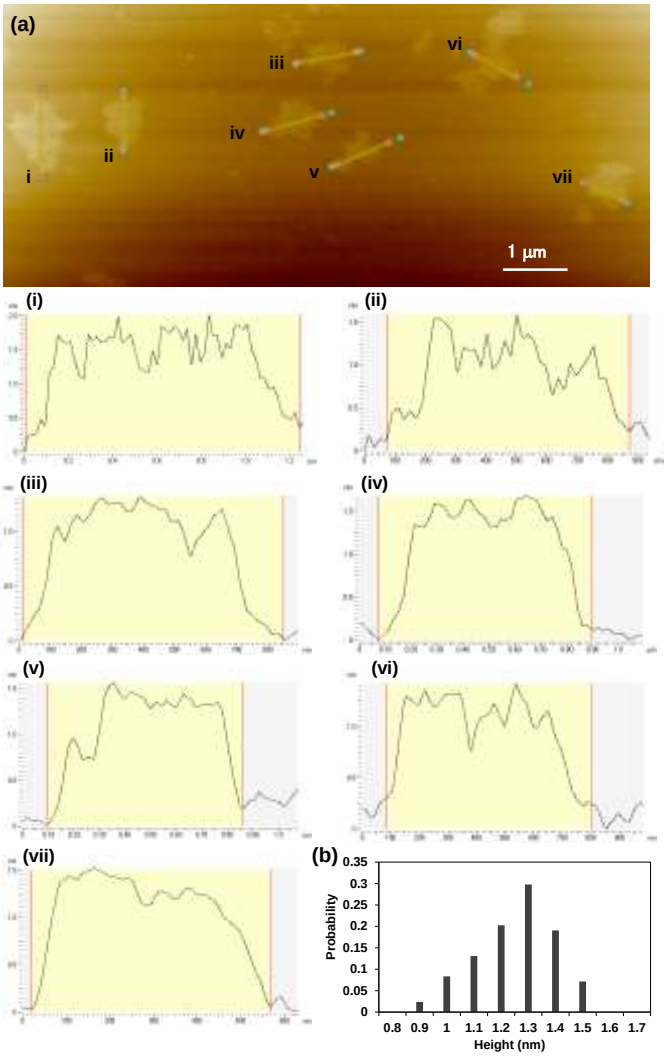

Fig. 5. (a) AFM images of eicosylated graphene **1l**, and (b) Histogram of feature heights of eicosylated graphene **1l** by AFM (84 flakes were measured).

3.3. Effect of absolute Na concentration

The same optimal C/Na ratio (C/Na = 12) was initially observed for dodecylated graphenes (Fig. 6a). At this charge ratio, the (002) diffraction peak of the dodecylated graphene is almost absent (Fig. 6a) and GR shows the highest value (Fig. 6b (●)). However, on varying the absolute concentration of the reaction, the optimal C/Na ratios were found to vary (Fig. 6b). The optimal C/Na ratios for graphite concentrations of 0.04 M and 0.02 M are 4 and 2, respectively. By replotting the data (Fig. 7a), it is clear that the absolute Na concentration is the critical parameter, with the same optimum (~0.01 M) for exfoliation and grafting of GIC at all graphite concentrations. Interestingly, the optimum corresponds to a calculated Debye length[37] of ~1.0 nm (Fig. 7b). From a practical point of view, high graphite concentrations are convenient for scaling; using the optimal sodium concentration, it was possible to graft at 0.3 M graphite (3.6 mg ml^{-1}) successfully (optimal C/Na ratio ~24 (Fig. 6b), [Na] = 0.013 M (Fig. 7a)). However, further increases in graphite concentration are prevented by the charge stoichiometry required[29] for the formation of stage-1 Na-THF-GIC ($Na(THF)_{3.5}C_{32}$). At C/Na ratio ~36 ([Na] = 0.008 M) (Fig. 6b) there is a dramatic reduction in grafting ratio.

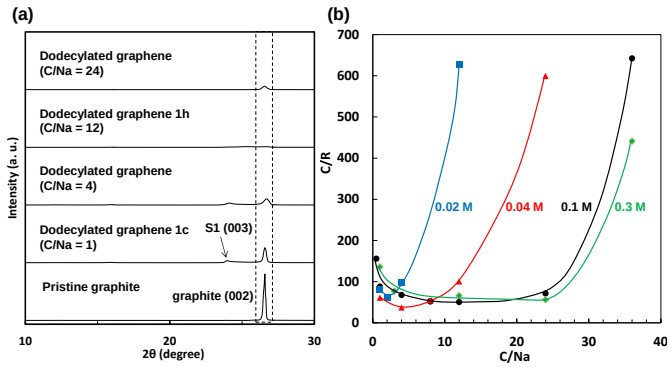

Fig. 6. (a) XRD patterns of pristine graphite and dodecylated graphenes (C/Na = 1, 4, 12, and 24), and (b) the effect of changing the graphite concentration in the reaction (0.1 M (the standard concentration) (●), 0.02 M (■), 0.04 M (▲), and 0.3 M (◆)) on the relation between C/Na and C/R of dodecylated graphenes.

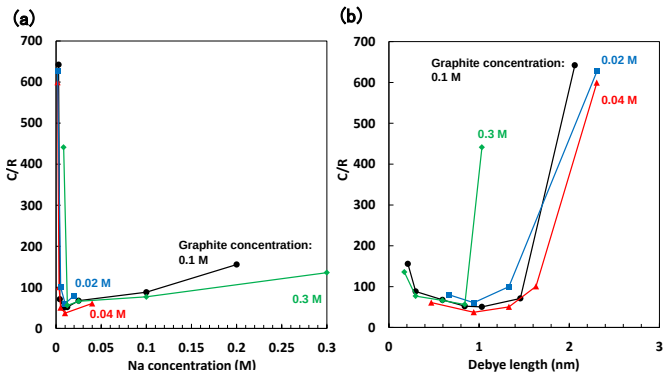

Fig. 7. (a) The relation between Na concentration in THF (graphite concentration is 0.1 M (●), 0.02 M (■), 0.04 M (▲), and 0.3 M (◆) respectively) and the C/R value of the obtained dodecylated graphenes, and (b) the relation between the Debye length and the C/R. The Debye length (κ^{-1}) for monovalent electrolytes between two charged surfaces was calculated by the equation[37]: $\kappa^{-1} = [\varepsilon\varepsilon_0 k_B T/2n_s e^2]^{1/2}$, where n_s is the bulk salt concentration in units of number density (m^{-3}), e is the elementary charge, k_B is the Boltzmann constant, T is the temperature, ε is the dielectric constant of THF, and ε_0 is the permittivity of free space.

3.4. Evaluation of solubility and yield

The solubility of the alkylated graphenes in solvents was evaluated, in DCB and chloroform, after short bath sonication for 10 min. A high initial concentration of alkylated graphene in each solvent, 1 mg ml^{-1} was selected to ensure saturation and hence obtain a measure of the maximum solubility (Fig. S6 shows the dependence on initial loading). The resulting dispersion was subjected to mild centrifugation (1,000 rpm, 5 min) to remove non-dispersed particles and yield a clear grey solution (Fig. 8). The UV-vis-NIR spectra of these supernatants showed featureless absorption (Fig. S7) as expected.[12,20] The concentration of each alkylated graphene supernatant was calculated using the extinction coefficient[12] for dispersed graphene in solution (α_{660} = 2,460 L g^{-1} m^{-1}). As shown in Fig. 8, long chain eicosylated graphene **1j** showed much higher solubility than either dodecylated (**1h**) or butylated (**1g**) graphene, despite its lower grafting density (high C/R). Eicosylated graphene **1j** has a higher grafted mass (23.0 wt%), as well as improved steric stabilisation due to the longer alkyl chains. Functionalisation using longer alkyl (eicosyl) chains is thus effective for improving solubility with minimum sp^2 disruption (low D/G ratio). In addition, the eicosylated graphene obtained at the optimal charge (**1j**) showed much higher solubilities than products obtained at higher charge (C/Na = 1) **1f** (Fig. 8, (△) and (○)). The optimised eicosylated graphene grafted after mild sonication to maximise exfoliation (**1l**) showed the best solubility (37 μg ml^{-1} in DCB and 20 μg ml^{-1} in chloroform). The optimal ratio consistently corresponds to a maximum dissolved yield of ~24 wt% of the original sample. Further washings with fresh DCB do not dissolve additional material; the remaining, undissolved alkylated graphenes are presumably physically trapped by entanglements or defects.

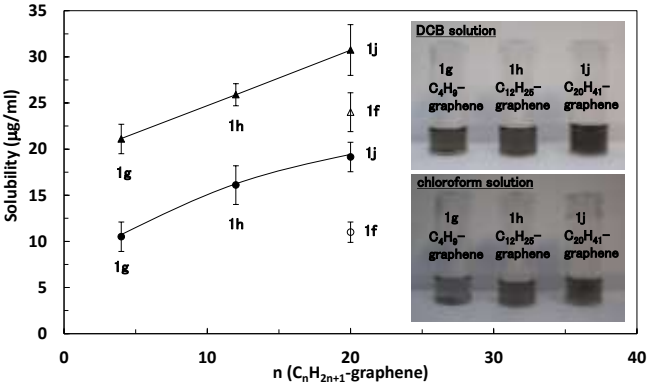

Fig. 8. Relation between the alkyl chain length of alkylated graphenes and their solubility (after mild centrifugation (1,000 rpm, 5 min) to remove non-dispersed particles). Alkylated graphenes (C/Na = 12) in DCB (▲) and chloroform (●), and alkylated graphenes (C/Na = 1) in DCB (△) and chloroform (○). Photographs show the supernatants of each alkylated graphene dispersion.

4. Conclusions

Isolated, soluble, alkylated monolayer graphenes were synthesised by reacting exfoliated Na-based GICs with alkyl halides. In this reaction, efficient exfoliation of the Na-reduced GICs into individually-dispersed graphenides provides accessible surface area for grafting by alkyl halides. Increasing the alkyl chain length led to large decrease of the GR, demonstrating that steric factors also play an important role. However, the use of an optimal sodium concentration (C/Na = ~12) dramatically improved exfoliation, increased the GRs, and enhanced solubility; the optimum balances total charge and charge condensation effects. The use of excess metal which may initiate unwanted side reactions, for example with solvent, can be avoided. Moreover, it was found that the absolute Na concentration is the critical parameter, with the same optimum (~0.01 M) for exfoliation and grafting of GIC at all graphite concentrations. High graphite concentrations are convenient for scaling; using the optimal sodium concentration, it was possible to graft even at high graphite concentration (0.3 M (3.6 mg ml^{-1})) successfully. In contrast to methods employing intense sonication or oxidation, this approach to synthesising modified graphenes limits defect formation to the relatively low concentration of sites required for grafting. The electrostatic and steric concepts described here can be applied to a wide range of electrophiles and to the charge-based exfoliation and functionalisation of other non-carbon analogues. Whilst more aggressive routes, such as the formation and reduction of graphene oxide, offer much higher solution concentrations, lower defect densities are needed to retain the intrinsic properties of interest, in many cases. The reduced metal requirement, minimal sonication, high graphite concentration, and rapid liquid phase reactions make this route appealing for

producing relatively large quantities of high quality functionalised graphenes for a variety of applications.

Acknowledgements

This work was supported by Toyota Central R&D Labs., Inc., Thomas Swan & Co. Ltd., and EPSRC (EP/G007314/1).

Notes and references

[a] Department of Chemistry, Imperial College London, London, SW7 2AZ, UK. Fax: +44 (0)2075945801; E-mail: m.shaffer@imperial.ac.uk

[b] Toyota Central R&D Labs., Inc., Nagakute, Aichi 480-1192, Japan.

Electronic Supplementary Information (ESI) available: supplementary figures. See DOI: 10.1039/b000000x/

1 S. Stankovich, D. A. Dikin, G. H. B. Dommett, K. M. Kohlhaas, E. J. Zimney, E. A. Stach, R. D. Piner, S. T. Nguyen and R. S. Ruoff, *Nature*, 2006, **442**, 282.

2 K. S. Novoselov, V. I. Fal'ko, L. Colombo, P. R. Gellert, M. G. Schwab and K. Kim, *Nature*, 2012, **490**, 192.

3 R. S. Edwards and K. S. Coleman, *Nanoscale*, 2013, **5**, 38.

4 H. Bai, C. Li and G. Shi, *Adv. Mater*., 2011, **23**, 1089.

5 X. Huang, X. Qi, F. Boey and H. Zhang, *Chem. Soc. Rev.*, 2012, **41**, 666.

6 Y. B. Tan and J. M. Lee, *J. Mater. Chem. A*, 2013, **1**, 14814.

7 D. Wei and J. Kivioja, *Nanoscale*, 2013, **5**, 10108.

8 H. Wang, K. Sun, F. Tao, D. J. Stacchiola and Y. H. Hu, *Angew. Chem. Int. Ed*. 2013, **52**, 9210.

9 P. W. Sutter, J.-I. Flege and E. A. Sutter, *Nat. Mater*., 2008, **7**, 406.

10 K. S. Kim, Y. Zhao, H. Jang, S. Y. Lee, J. M. Kim, K. S. Kim, J.-H. Ahn, P. Kim, J.-Y. Choi and B. H. Hong, *Nature* 2009, **457**, 706.

11 J. Cai, P. Ruffieux, R. Jaafar, M. Bieri, T. Braun, S. Blankenburg, M. Muoth, A. P. Seitsonen, M. Saleh, X. Feng, K. Müllen and R. Fasel, *Nature*, 2010, **466**, 470.

12 Y. Hernandez, V. Nicolosi, M. Lotya, F. M. Blighe, Z. Sun, S. De, I. T. McGovern, B. Holland, M. Byrne, Y. K. Gun'ko, J. J. Boland, P. Niraj, G. Duesberg, S. Krishnamurthy, R. Goodhue, J. Hutchison, V. Scardaci, A. C. Ferrari and J. N. Coleman, *Nat. Nanotechnol*., 2008, **3**, 563.

13 H. Wang and Y. H. Hu, *Ind. Eng. Chem. Res*. 2011, **50**, 6132.

14 H. Wang and Y. H. Hu, *J. Colloid Interface Sci*. 2013, **391**, 21.

15 A. A. Green and M. C. Hersam, *Nano Lett*., 2009, **9**, 4031.

16 U. Khan, A. O'Neill, M. Lotya, S. De and J. N. Coleman, *Small*, 2010, **6**, 864.

17 N. Behabtu, J. R. Lomeda, M. J. Green, A. L. Higginbotham, A. Sinitskii, D. V. Kosynkin, D. Tsentalovich, A. N. G. Parra-Vasquez, J. Schmidt, E. Kesselman, Y. Cohen, Y. Talmon, J. M. Tour and M. Pasquali, *Nat. Nanotechnol*., 2010, **5**, 406.

18 E. M. Milner, N. T. Skipper, C. A. Howard, M. S. P. Shaffer, D. J. Buckley, K. A. Rahnejat, P. L. Cullen, R. K. Heenan, P. Lindner and R. Scheins, *J. Am. Chem. Soc*., 2012, **134**, 8302.

19 a) C. Vallés, C. Drummond, H. Saadaoui, C. A. Furtado, M. He, O. Roubeau, L. Ortolani, M. Monthioux and A. Pénicaud, *J. Am. Chem. Soc.*, 2008, **130**, 15802; b) A. Catheline, C. Vallés, C. Drummond, L. Ortolani, V. Morandi, M. Marcaccio, M. Iurlo, F. Paoluccic and A. Pénicaud, *Chem. Commun*., 2011, **47**, 5470.

20 J. M. Englert, C. Dotzer, G. Yang, M. Schmid, C. Papp, J. M. Gottfried, H.-P. Steinrück, E. Spiecker, F. Hauke and A. Hirsch, *Nat. Chem*., 2011, **3**, 279.

21 J. M. Englert, K. C. Knirsch, C. Dotzer, B. Butz, F. Hauke, E. Spiecker and A. Hirsch, *Chem. Commun*., 2012, **48**, 5025.

22 K. C. Knirsch, J. M. Englert, C. Dotzer, F. Hauke and A. Hirsch, *Chem. Commun*., 2013, **49**, 10811.

23 F. Liang, A. K. Sadana, A. Peera, J. Chattopadhyay, Z. Gu, R. H. Hauge and W. E. Billups, *Nano Lett*. 2004, **4**, 1257.

24 S. Chakraborty, J. Chattopadhyay, W. Guo and W. E. Billups, *Angew. Chem. Int. Ed.*, 2007, **46**, 4486.

25 G. S. J. Manning, *Chem. Phys*. 1969, **51**, 924.

26 D. Voiry, C. Drummond and A. Pénicaud, *Soft Matter*, 2011, **7**, 7998.

27 S. Fogden, C. A. Howard, R. K. Heenan, N. T. Skipper and M. S. P. Shaffer, *ACS Nano*, 2012, **6**, 54.

28 M. Inagaki and O. Tanaike, *Synth. Met*., 1995, **73**, 77.

29 T. Enoki, M. Suzuki and M. Endo, *Graphite Intercalation Compounds and Applications*; Oxford University Press, 2003, pp. 30.

30 A. C. Ferrari, J. C. Meyer, V. Scardaci, C. Casiraghi, M. Lazzeri, F. Mauri, S. Piscanec, D. Jiang, K. S. Novoselov, S. Roth and A. K. Geim, *Phys. Rev. Lett.*, 2006, **97**, 187401.

31 V. Damien, O. Roubeau and A. Pénicaud, *J. Mater. Chem*., 2010, **20**, 4385.

32 R. A. Schäfer, J. M. Englert, P. Wehrfritz, W. Bauer, F. Hauke, T. Seyller and A. Hirsch, *Angew. Chem. Int. Ed*., 2013, **52**, 754.

33 K. Inoue, K. Okamoto, N. Ogui, H. Ochiai, T. Sato, H. Yasuda and Y. Yamashita, *Kobunshi Kagaku*; Asakura shoten, 1994, pp. 143.

34 S. Niyogi, E. Bekyarova, M. Itkis, H. Zhang, K. Shepperd, J. Hicks, M. Sprinkle, C. Berger, C. Lau, W. Deheer, E. Conrad and R. C. Haddon, *Nano Lett*. 2010, **10**, 4061.

35 K. S. Novoselov, A. K. Geim, S. V. Morozov, D. Jiang, Y. Zhang, S. V. Dubonos, I. V. Grigorieva and A. A. Firsov, *Science*, 2004, **306**, 666.

36 A. Srivastava, C. Galande, L. Ci, L. Song, C. Rai, D. Jariwala, K. F. Kelly and P. M. Ajayan, *Chem. Mater*., 2010, **22**, 3457.

37 R. Tadmor, E. Hernández-Zapata, N. Chen, P. Pincus and J. N. Israelachvili, *Macromolecules*, 2002, **35**, 2380.